Fracture Mechanics of Concrete and Concrete Structures -
Recent Advances in Fracture Mechanics of Concrete - B. H. Oh, et al.(eds)
ⓒ 2010 Korea Concrete Institute, Seoul, ISBN 978-89-5708-180-8

Early-age cracking in massive concrete structures: an active ring test to study the effects of reinforcement and construction joints

M. Briffaut
LMT/ENS Cachan/CNRS UMR8535/UPMC/PRES UniverSud Paris, Cachan, France
Institut de radioprotection et de sûreté nucléaire, Fontenay-aux-Roses, France

F. Benboudjema
LMT/ENS Cachan/CNRS UMR8535/UPMC/PRES UniverSud Paris, Cachan, France

G. Nahas
Institut de radioprotection et de sûreté nucléaire, Fontenay-aux-Roses, France
LMT/ENS Cachan/CNRS UMR8535/UPMC/PRES UniverSud Paris, Cachan, France

J.M. Torrenti
Université Paris Est, Laboratoire central des ponts et chaussées, Paris, France

ABSTRACT: At early-age in massive concrete structures, cracking may occur during hardening. This cracking may increase significantly the concrete permeability and thus increase leakage (tank, nuclear containment,…) and reduce the durability. The restrained shrinkage ring is a good test to determine the early-age concrete behavior (creep strain and cracking) due to the autogenous and drying shrinkage. This test shows that at 20°C and without drying, the amplitude of autogenous shrinkage is not high enough to cause cracking (for our concrete mix which is representative of nuclear power plant containment). Indeed, in this configuration, thermal shrinkage does not occur. Therefore, a new test has been developed to study cracking due to restrained thermal shrinkage. This new test is an evolution of the restrained shrinkage ring test which allows to take into account the autogenous shrinkage and also the thermal shrinkage. With this test, the early age cracking due to restrained shrinkage and the influence of reinforcement and construction joints have been studied.

1 INTRODUCTION

At early-age in massive concrete structures, cracking may occur during hardening. Indeed, hydration is an exothermic chemical reaction (temperature in concrete may overcome 60°C). Therefore, if autogenous and thermal strains are restrained (self restrainement, construction joints), compressive stresses and then tensile stresses rise, which can exceed the concrete strength (in an elastic finite element calculation) and induce cracking in a real structure. For structures like tanks or nuclear containments, this cracking may increase significantly the concrete permeability and reduce the tightness.

The restrained shrinkage ring is a good test to determine the concrete behavior (creep strain and cracking) due to the autogenous and drying shrinkage. In this study, a concrete mix which is representative of the one of nuclear power plant containment (the width of concrete is equal to 1.2m) is tested. This test showed that at 20°C and in endogenous conditions (without drying, cf. Fig. 1), the amplitude of autogenous shrinkage is not high enough to cause cracking. Indeed, in this configuration, thermal shrinkage does not occur. Therefore, a new device (devoted to be representative of a massive structure) has been developed to study the cracking due to restrained thermal shrinkage in laboratory conditions.

2 NEW TEST PRESENTATION

This new test is an evolution of the restrained shrinkage ring test which allows to take into account the autogenous shrinkage and also the thermal shrinkage.

2.1 *"Classical" restrained shrinkage ring test presentation*

The "classical" ring test was initially designed to observe the cracking of a concrete ring specimen which is cast around a rigid core (generally in steel): only the cracking age was accessible and the stresses generated by restrained shrinkage could not be deduced. Then, Pailliere and Serrano (1976) and Swamy and Starvides (1979) optimized the ring dimension and added instrumentation in order to measure strains on the steel ring. Finally, Grzybowski and Shah (1989) placed strain gages on the steel ring in order to deduce the stresses in the concrete ring. This test configuration offers several advantages and particularly the fact that the stresses are self generated by restrained shrinkage and specimen geometry. Indeed, no additional complex load system is needed (Fig. 1: Ring test geometry for concrete). Actually, in our laboratory the brass is preferred to the steel to prevent chemical reaction between the metallic ring and the concrete.

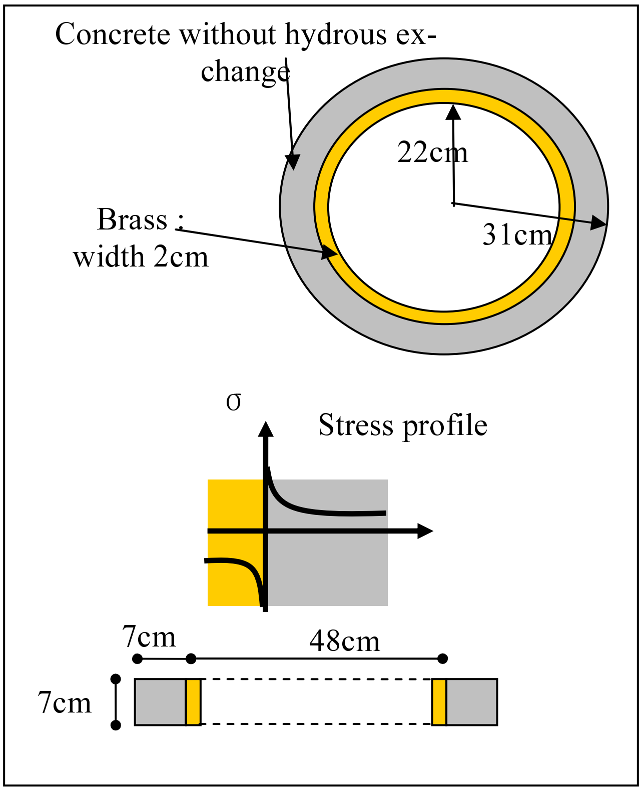

Figure 1. "Classical" Ring test geometry.

2.2 *"Classical" restrained shrinkage ring test results*

A concrete mix representative of a nuclear power plant containement has been tested. The cement used is a composed Portland cement (French ref.: CEM II/A-LL 42,5 R CE PM-CP2).

Table 1. Composition of our concrete mix.

		1 m^3
Ciment	kg/m^3	350
Sand (0-5 mm)	kg/m^3	772
g (5-12,5 mm)	kg/m^3	316
G (12,5-20 mm)	kg/m^3	784
Water	L/m^3	201
Superplasticizer	L/m^3	1,225

Figure 2 shows the temperature evolution measured during the classical test and on Figure 3, one can observe the stresses evolution in both materials.

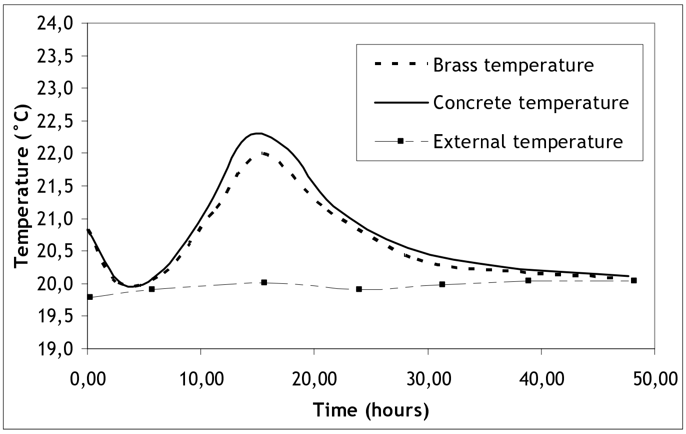

Figure 2. Temperature evolution during the "classical" restrained ring test.

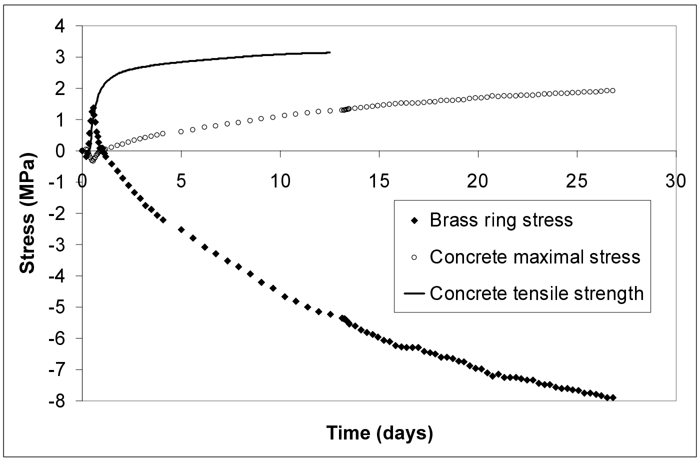

Figure 3. Stresses evolution during the "classical" restrained ring test.

The conclusion of this first test is that no macroscopic crack in the concrete ring was obtained because the stresses generated by the restrained autogenous shrinkage do not exceed the concrete tensile strength (cf Fig. 3). In fact, in this test, the specimen is not massive enough to represent the thermal evolution of a massive structure. Consequently, the effect of thermal shrinkage is negligible in this test. Note that the stresses in the brass and in the concrete ring are calculated from the brass strains (measured by strains gages placed on the inner radius of the brass ring) with the formula given by Hossein and Weiss (2004). This highlights the need to develop an adapted device for massive concrete structure which is presented below.

2.3 *An active restrained shrinkage ring test*

The new test aims to predict the behavior and the cracking at early age of massive structures (like nuclear power plant containment). The new test principle is to increase the temperature of the brass ring in order to expand it. In this case, the expansion of the ring is restrained by the extern concrete layer (the thermal dilatation coefficient of the brass is about 3 times higher than the concrete one). This induces compressive stresses in the ring and therefore tensile stresses in concrete. The temperature evolution of the brass ring is imposed by the water circulation into the ring (Figs. 4-5) and the brass ring strains are measured by 3 strains gages placed at 120°.

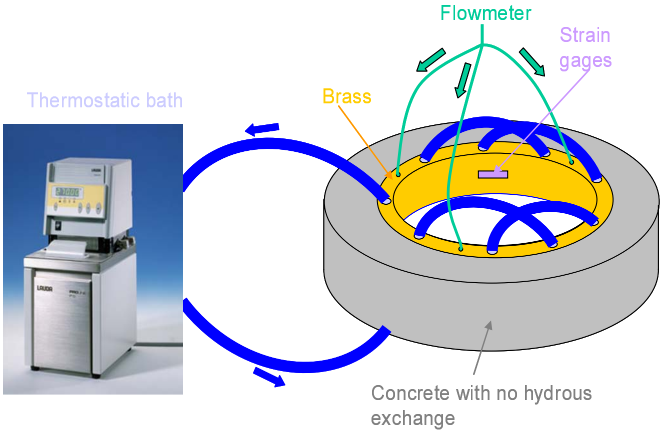

Figure 4. Active ring test geometry scheme.

The device also allows us to measure the permeability of the concrete ring by radial air injection. Moreover, temperature sensors (thermocouples type J) are placed on the internal radius of the brass ring and on the middle of the concrete section.

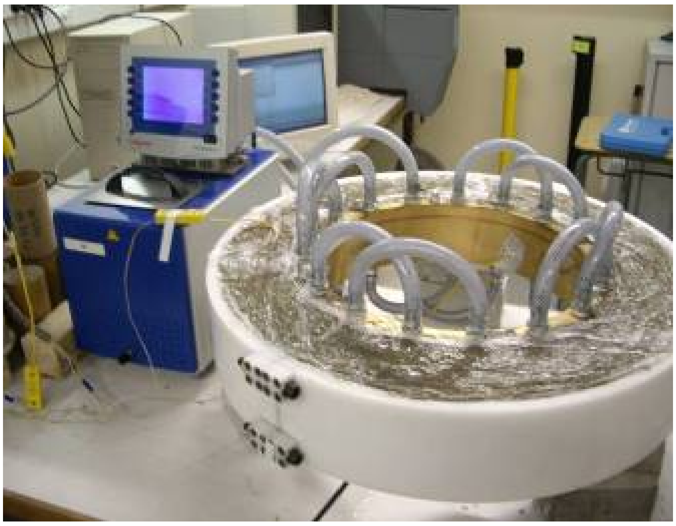

Figure 5. New ring test.

The new test objectives are to reproduce a similar stress history that the one which occurs in a “real’ massive wall (calculated by means of finite element simulations or from experimental temperature data: Ithurralde (1989), cf. Figs. 6-7).

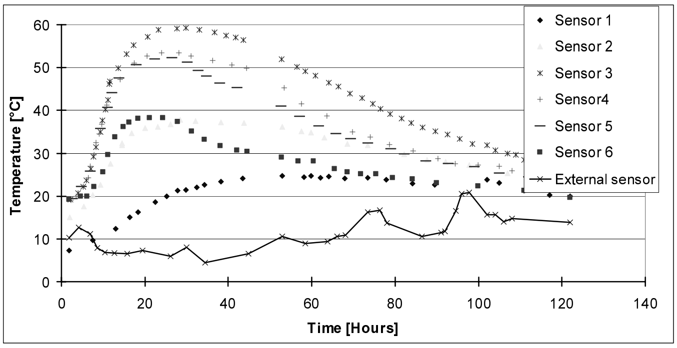

Figure 6. History of temperature measured in a concrete wall (1.2 m width).

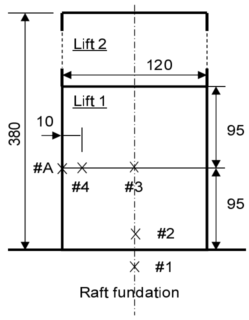

Figure 7. Geometry of the wall and location of the temperature sensors.

The specimen dimensions in the active ring test have been increased to obtain a concrete ring section of 10cm x 10cm. Indeed, the maximal aggregate size of our mix is about 20mm, and the section of the ring presented in the first part of this article (7cm x 7cm) is not sufficient to obtain a representative concrete section. Moreover, reinforced concrete is also studied and a smaller section cannot guarantee a representative covering of a real structure. The dimensions of the brass ring (the internal radius and the ring width) have been calculated to obtain measurable strains in the ring (strains gages accuracy is about 5µm/m) but also to stay in a reasonable range of weight: 19cm for the internal radius and 3cm for the ring width. Because in massive structure, drying is 1000 to 10 000 times slower than heat transfer, at early age massive structures are in endogenous conditions (except the external concrete skin). That is why, our tests are performed with no hydrous exchange with the environment. To prevent this exchange, the concrete ring is covered by an adhesive aluminum layer (the weight loss is inferior to 0, 1% after 7 days).

A simpler device would have consisted in the insulation of the concrete ring. However, with this solution, the cracking would occur during the temperature increase (because the thermal dilatation coefficient of brass is higher than the concrete one) and not during the decrease like in reality.

It should be noticed that this device is well adapted to describe cracking during concrete lift, but cannot retrieve thermal stresses due to self restraint (temperature gradient inside the thickness). However, numerical simulation show that, for the studied concrete, thermal stresses due to self restrain do not lead to cracking.

3 ACTIVE RESTRAINED SHRINKAGE RING TEST NUMERICAL VALIDATION

In order to optimize the ring geometry and to check that cracks rise in concrete with this device the numerical model described in Benboudjema, Torrenti, (2008) has been used.

The temperature evolution is obtained by solving the heat equation with a thermal source term ($L\dot{\xi}$), corresponding to the release of heat during hydration:

$$C\dot{T} = \nabla(k\nabla T) + L\dot{\xi}$$

where C is the volumic thermal capacity [J.m-3.K-^{1}] which can be kept constant according to Waller (2000), T is the temperature [K], k is the thermal conductivity [W.m^{-1}.K^{-1}] which can be kept constant according to Mounanga (2003), L is the total heat release [J.m^{-3}] and ξ is the hydration degree [-].

The model takes into account the thermal and autogenous strains but also the basic concrete creep. Finally, an isotropic damage model based on Mazars (1986) model is used. The adaptation for the early age consists in the dependency of the damage threshold to the hydration degree:

$$\kappa_0(\xi) = \frac{f_t(\xi)}{E(\xi)} = \frac{f_t(\xi_\infty)}{E(\xi_\infty)}(\xi - \xi_0)^{\gamma-\beta}$$

where γ and β are the coefficients of respectively tensile strength and Young modulus evolution (De Schutter, 96, 97, 99), ξ is the hydration degree [-], ξ_∞ is the final hydration degree [-], ξ_0 is the percolation threshold [-], κ_0 is the mechanical strain threshold [-], ft is the tensile strength [MPa], E is the Young modulus [GPa].

An example of damage field is display on fig. 8 (creep is not taken into account), where several cracks are to be noticed. Similar results are obtained if creep is taken into account.

Figure 8. Damage field (creep is not taken into account). Mesh: ¼ of the ring.

Therefore, this test may be used to test the sensibility of concrete to thermal cracking.

4 ACTIVE RESTRAINED SHRINKAGE RING TEST EXPERIMENTAL RESULTS

4.1 *Analysis of the experimental results*

The brass ring and the concrete temperatures are measured by thermocouples (Fig. 9) and the brass ring strains are measured by three strain gages on the internal radius of the ring (Fig. 10).

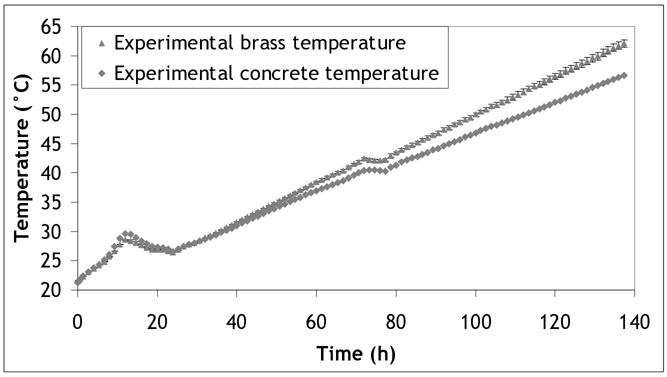

Figure 9. New ring test temperature evolution.

Although the temperature is punctually imposed by the fluid circulation in this test, the Figure 9 shows that a quite homogeneous temperature in the ring is obtained (the two temperature probes are placed opposite on the same diameter). At the beginning of the test (first 24h), the temperature increase is due to the hydration reaction. Then, the temperature rise is imposed by the thermostatic bath with a rate of 0.35°C/h. Near the middle of the test, a stable period at 42.8°C allows us to verify that the device doesn't have too much inertia.

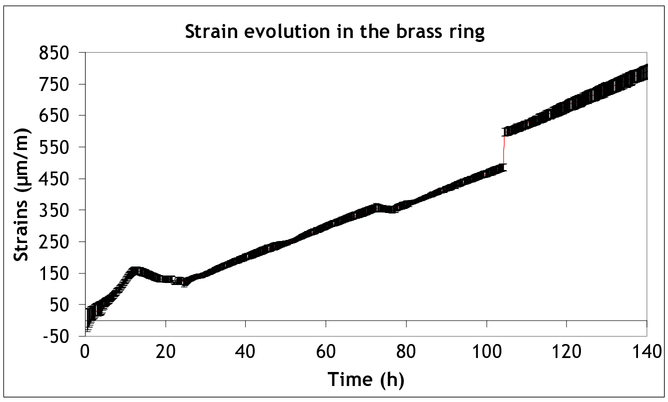

Figure 10. New ring test strains evolution.

The brass strains are corrected to take into account the strain gage thermal dilatation. The first result is that we effectively obtained an experimental crack (Fig. 11) on this test which correspond to a gap in the strains evolutions (Fig. 10). Crack occurs for a brass ring temperature value of 51.5°C (experimental crack width was about 650µm). Moreover, the brass ring solicitations seem to be uniform because the three strain gages measures are quite similar.

At the beginning of the test, the strain evolution is due to the temperature evolution of the system. Then, when the brass ring temperature is imposed by the fluid circulation, the ring strain is a combination of the brass ring and the concrete ring thermal dilatation. Indeed the thermal dilatation coefficient of the brass is about 3 times higher than the concrete one, therefore tensile stresses rise in the concrete ring. When the concrete tensile stress exceeds the concrete tensile strength, crack occurs.

In this test, it is really interesting to note that only one crack is obtained and that it is a crossing crack. Effectively, the crack crosses the entire concrete specimen section and furthermore, this crack crosses the concrete aggregates.

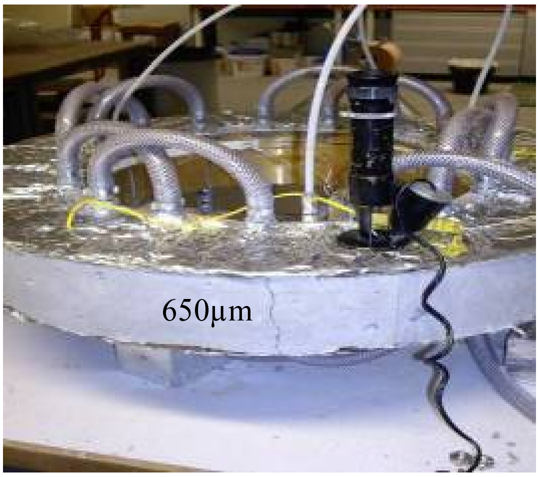

Figure 11. Experimental crack picture.

5 REINFORCEMENT AND CONSTRUCTION JOINTS EFFECT

In a real massive structure, concrete is reinforced by steel bars. Moreover, massive elements cannot be cast in one time and construction joints are needed. The effect of the steel bar and the construction joints are not similar because the steel bars tends to distribute the cracks and to limit the crack opening whereas the construction joints tends to decrease the homogeneity of the massive structure and to create weakness areas. That's why, the influence of each parameter has been studied.

5.1 *Steel bars effect*

To study the effect of steel bars on the new test we placed in the middle of the concrete section two 8mm diameter steel bars. In order to guarantee the stress continuity in the steel bar and to avoid any recovering length we weld the steel bars to obtain steel rings (see Fig. 12)

Figure 12. Ring reinforcement.

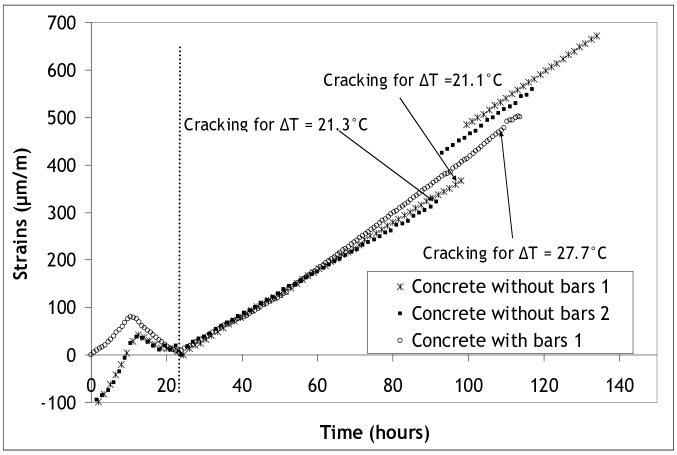

Figure 13. Active ring test strains evolution (for reinforced concrete).

The mechanical results obtained are presented in Figure 13. It represents the evolution of the brass strains. In this graph, the strains have been reinitialized at the beginning of the temperature increase (time when the temperature is imposed by the hot water circulation). It shows that the concrete crack is obtained later than for the concrete without bars. Effectively, the crack is obtained for a temperature increase of 27.7°C (the reference correspond to the time when the temperature is imposed by the hot water circulation) whereas the temperature increase for the concrete without bars is about 21°C. Moreover the strain gap on the strain evolution is lower compared to the gap obtained with a ring without steel bars. That indicates that the crack opening is limited by the presence of steel bar which can be also observed experimentally on Figure 14 (the cracks opening is equal to about 100µm whereas the crack opening in the test without bars was equal to about 650µm).

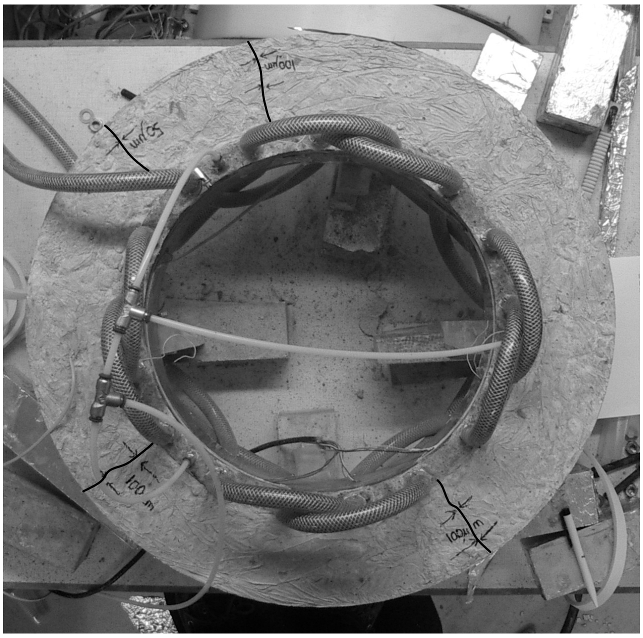

Figure 14. Location of cracks in the reinforced concrete ring bar at the end of the test.

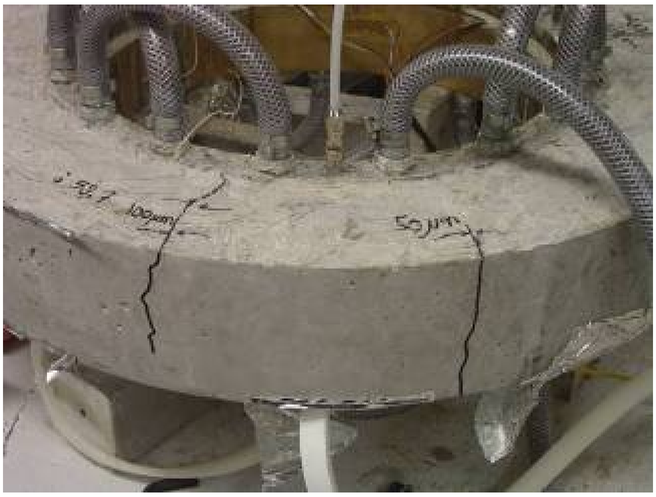

Figure 15. Complementary cracks.

Finally, we can also deduce from this test that the steel bars distribute the cracking because more than one crack are obtained. On Figure 14, four cracks can be observed. Among these, two of them are crossing cracks, whereas the two other ones are not (Fig. 15).

5.2 *Construction joints effect*

To study the influence of the construction joints on the early age behavior of massive structures we cast a concrete ring in two parts. The first part is composed by two quarters of the ring placed on the same diameter and the second part is composed by the two other parts of the ring (Fig. 16). The second part is cast 2 weeks later than the first one. Thus, we obtain a complete ring with four construction joints.

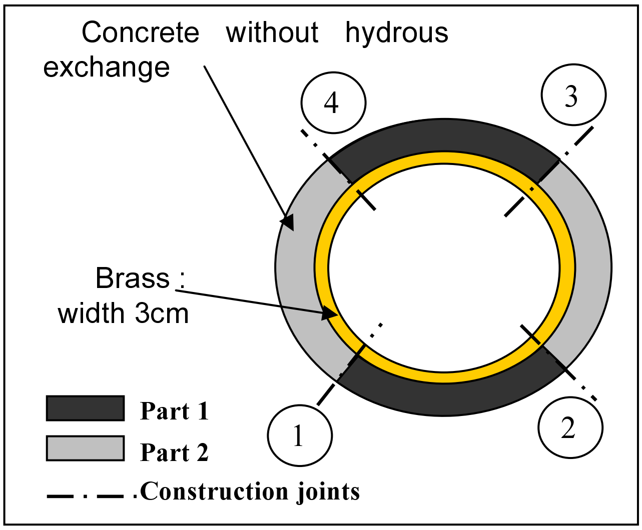

Figure 16. Scheme of the cast partition for the ring with construction joints.

To obtain a roughness of the surface which is representative of the surface state of massive structure construction joints, the surfaces between the two parts of the ring have been mechanically scraped (Fig. 17). The results of the test are presented on Figure 18.

Figure 17. Surface state for the construction joints.

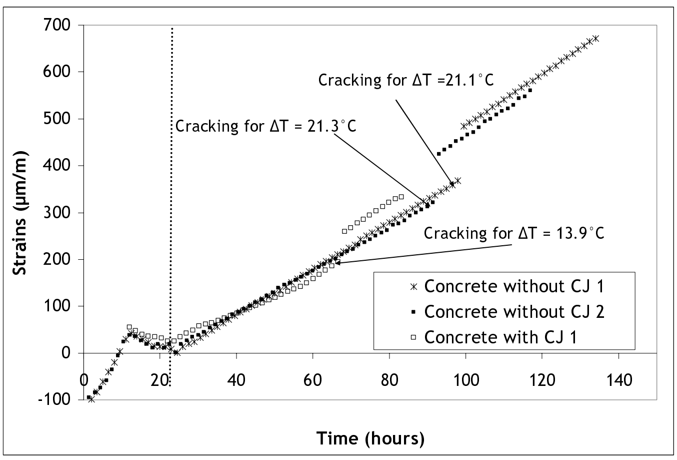

Figure 18. Strains evolution (CJ = construction joints).

On this graph, the strains have also been reinitialized at the beginning of the temperature increase (see §5.1). It shows that the concrete crack is obtained earlier than for the concrete without construction joints. It is interesting to note that the benefit from the addition of steel bars on the time of cracking (about 7°C) is approximately the same than the loss lead by the construction joints.

The Figure 19 represents the cracking pattern. In this test only one crack at one construction joint is obtained and its width is about 550µm. This crack opening is nearly the same than for the concrete with no steel bar and no construction joint, given the fact that the cracking temperatures are not the same.

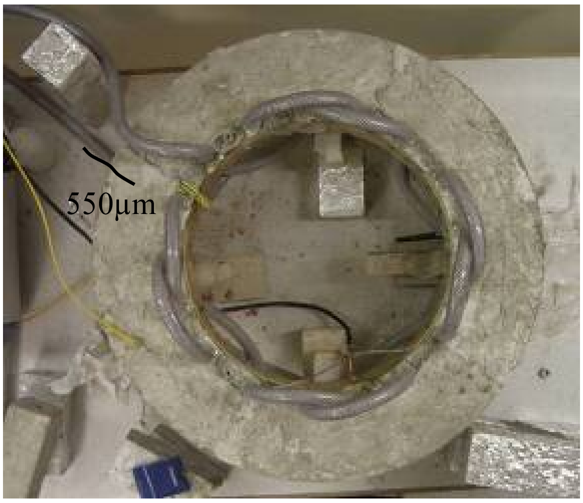

Figure 19. Ring with construction joints at the end of the test.

This study shows that the effects of the construction joints are very important and harmful for the mechanical strength of concrete, especially in tension. That is why, they have to be taken into account (and all the construction stage) in the modeling of massive elements. Otherwise, long term performance could be widely overestimated.

6 CONCLUSION

In this study, an active device to study the early age behavior and cracking of massive structure has been developed. This new test was needed because the classical restrained ring test did not take into account the thermal strains. So it was not able to reproduce realistic stresses which can occur in massive structures. With this active test we are allowed to study early age concrete cracking.

The active device is an evolution of the restrained shrinkage ring test. The thermal strain effects are created by an expansion of the brass ring to reproduce the stress rate of a real massive structure. The expansion of the ring is obtained by the circulation of hot water into the brass ring.

Firstly, a numerical validation of the test was achieved and shows that cracks should be obtained for suitable value of temperature. Then, the new test was performed and cracking was experimentally obtained.

Secondly, a study on the effect of steel bars reinforcement and construction joint was performed with this new device. The results showed that the effect of steel bar are multiple (cracking is delayed, cracking opening are reduced and cracks are distributed). They also corroborate the fact that construction joints reduce considerably the strength of the concrete element and highlight the fact that they must be taken into account in the modeling of massive structure.

The next step is to study the permeability evolution of the concrete ring due to the early age cracking. Furthermore, the numerical model (which is not able at this point to predict the occurrence of only one crack) is being improved : variability of materials parameters and interface elements between concrete and brass are being added.

REFERENCES

Benboudjema, Torrenti, 2008 Early-age behaviour of concrete nuclear containments, Nuclear Engineering and Design, Volume 238, Issue 10, Pages 2495-2506

Commissariat à l'Energie Atomique CEA - DEN/DM2S/SEMT, Cast3m finite element code, available at http://www-cast3m.cea.fr/

De Schutter G, Taerwe L (1996), Degree of hydration based description of mechanical properties of early-age concrete, Materials and Structure, 29, pp335-344

De Schutter G., Taerwe L. (1997), Fracture energy of concrete at early ages, Materials and Structures, 30, p. 67-71

De Schutter G. (1999), Degree of hydration based Kelvin model for the basic creep of early age concrete, Materials and Structures,32, p. 260-265.

Grzybowski, Shah, (1989) Model to predict cracking in fiber reinforced concrete due to restrained shrinkage. Mag Concrete Res, 41 :125–135

Ithurralde G. (1989), La perméabilité vue par le maître d'ouvrage, Colloque Béton à hautes performances, Ecole Normale Supérieure, Cachan, 1989.

Mazars J. (1986) A description of micro and macroscale damage of concrete structures, Engineering Fracture Mechanics, 25(5:6), p. 729-737.

Mounanga P. (2003), Etude expérimentale du comportement de pâtes de ciment au très jeune âge, PhD Thesis, in French

Paillère, Serrano, (1976). Appareil d'étude de la fissuration du béton. Bulletin de liaison du Laboratoire Centrale des Ponts et Chaussées n.83, Laboratoire Centrale des Ponts et Chaussées

Swamy, Starvides, (1979) Influence of fibber reinforcement on restrained shrinkage and cracking. ACI Journal proceedings, 76[3] :443–460

Waller V., (2000) « Relations entre composition des bétons, exothermie en cours de prise et résistance en compression », collection Etudes et recherches des Laboratoires des Ponts et Chaussées, série « Ouvrages d'Art », OA35 – LCPC, Paris, in French.